Research Square

Preprints are preliminary reports that have not undergone peer review.
They should not be considered conclusive, used to inform clinical practice,
or referenced by the media as validated information.

Diffusion brazing using powder mixtures of the CoCrFeNi MEA and low melting additives

Laura Bültena
TU Dortmund University: Technische Universitat Dortmund
Merle Hansen
TU Dortmund University: Technische Universitat Dortmund
Wolfgang Tillmann
TU Dortmund University: Technische Universitat Dortmund
Lukas Wojarski
lukas.wojarski@tu-dortmund.de

TU Dortmund University: Technische Universitat Dortmund https://orcid.org/0000-0002-3698-4596

Research Article

Keywords: high entropy alloy, TLP, high-vacuum brazing, stainless steel, brazing, melting point depressants

Posted Date: October 31st, 2026

DOI: https://doi.org/10.21203/rs.3.rs-11062318/v1

License: This work is licensed under a Creative Commons Attribution 4.0 International License.
Read Full License

Abstract

Conventional nickel-based filler alloys for brazing commonly require low melting elements like boron or phosphorus to reduce the required brazing temperature. However, these elements often promote the formation of brittle intermetallic compounds (IMC), which can significantly reduce the joint strength. The reduction in strength is strongly dependent of the gap width as it influences the ratio of melting point depressing elements content to the faying surface area. This leads to a limitation of the maximum applicable joint gap. High entropy alloy (HEA) filler alloys could be an innovative engineering solution to overcome the technical restriction and to produce strong joints even with wider mounting gaps. This can be attributed to the tendency of HEA to form stable solid solutions that feature a high thermal and chemical stability instead of forming brittle intermetallic compounds. Therefore, it is expected that a HEA microstructure in the brazed metal leads to an improvement of the mechanical properties of the brazed joint. Unfortunately, HEA tend to have high melting temperatures, which impedes their application as brazing filler alloy. Therefore, this study presents a novel approach, in which a medium entropy alloy (MEA) consisting of pre alloyed CoCrFeNi-powder is mixed with various melting point depressants (MPDs), which melts at the brazing temperature and forms a HEA microstructure during isothermal solidification. The influence of different MPD concentrations and brazing temperatures on the resulting joint microstructure were analyzed and evaluated.

1 Introduction

The performance and quality of a brazed joint depends to a large extent on the selection of an appropriate filler alloy. For the manufacture of joints subjected to high thermal and mechanical stresses, commonly fillers on nickel- or iron-base are used, particularly when brazing under high vacuum at elevated temperature is the production technique. These brazing alloys have been widely used in industry and are therefore well researched [1].

Conventional nickel-based filler alloys contain melting-point depressants such as boron, silicon or phosphorus. However, these elements tend to form brittle intermetallic compounds, which can reduce the mechanical strength and negatively affect the long-term durability. The brittle intermetallic phases can be observed both as finely disperse particles and as a continuous hard-phase band within the center of the brazing gap. [2, 3]

An innovative method in the field of brazing involves using high-entropy alloys (HEAs) as brazing materials. Unlike conventional alloys, HEAs are recognized for their high thermal stability, high hardness, and excellent resistance to wear and corrosion [4]. These outstanding properties can be attributed to the high entropy effect within this material class that enhances the formation and stabilization of a single solid solution that impedes the formation of usually brittle intermetallic phases. For these reasons, HEA can be used wherever conventional brazing alloys reach their limits [5–8]. By definition, high-entropy alloys (HEAs) are comprised of a single solid solution that consist of at least five principal elements, each with a concentration between 5 and 35 at.-% [9]. In addition to this compositional criterion, HEAs

can also be classified based on their configurational entropy. Assuming ideal mixing and considering the maximization of the entropy of mixing, alloys with a configurational entropy of $\Delta S_{conf} > 1.5R$ are generally classified as HEAs, where *R* denotes the universal gas constant. In contrast, alloys with $\Delta S_{conf} < 1.0R$ are referred to as low-entropy alloys (LEAs), while alloys with configurational entropy values in the range of $1.0R < \Delta S_{conf} < 1.5R$ are classified as medium-entropy alloys (MEAs). The configurational entropy can be calculated according to Eq. (1). [10]

$$\Delta S_{conf} = -R \sum_{i=1}^{n} x_i ln x_i$$

1

R represents the universal gas constant, which is 8.314 J/K mol, x_i is the molar fraction of the element i and S_{conf} is the configuration entropy.

In equimolar mixtures the configuration entropy reaches its maximum value and increases logarithmically with the numbers of alloying elements as it is shown in Eq. (2). [9]

$$\Delta S_{conf} = R \ln n$$

2

In this equation n represents the number of the alloying elements. HEA are also subject to various thermodynamic effects that depend on configuration entropy and mixture entropies.

When using HEA as a brazing alloy, its high mixing entropy is exploited. The high mixing entropy and the distorted lattice structure—which results in sluggish diffusion—makes HEAs an attractive choice for brazing applications in which conventional brazing alloys reach their limitation. In particular, HEA is said to suppress the formation of brittle phases, enhance thermodynamic stability, and allow excellent adaptability to different base materials through compositional tailoring. Furthermore, the high mixing entropy promotes the formation of a stable solid-solution structure, resulting in a more homogeneous microstructure within the brazed joint and consequently reducing embrittlement [8, 9].

Various high-entropy alloys (HEAs) have already been investigated as brazing alloys for high-temperature joining applications. Bridges et al. examined a NiCoCuMnFe HEA as a brazing alloy for laser brazing, using the nickel-based superalloy IN718 as the base material [11]. The combination of the HEA brazing alloy and the IN718 base material resulted in the formation of a single-phase face-centered cubic (FCC) HEA brazed joint, which exhibited a maximum shear strength of 220 MPa at a brazing temperature of 1165°C.

Similarly, Tillmann et al. investigated the joining of Crofer 22 APU and hafnium-metallized yttria-stabilized zirconia (YSZ) using the compositionally complex alloy $Nb_{0.73}CoCrFeNi_{2.1}$ as a brazing alloy [12]. Brazing was performed at a process temperature of 1200°C with a holding time of 5 min. The eutectic microstructure, consisting of a solid-solution phase and a C14 Laves phase, exhibited high

thermal stability during the brazing process. Although hafnium diffusion led to grain coarsening, no phase transformation was observed, indicating excellent microstructural stability of the brazing alloy under the applied joining conditions.

Unfortunately, the melting range of HEA usually lies significantly above the working temperature of nickel-based filler alloys and the addition of melting point depressing elements like gallium, tin or germanium do not lead to a significant drop of the melting range [13, 14]. Therefore, no direct substitution of nickel-based filler alloys is possible. One promising strategy to overcome this obstacle is to add the melting point depressant as additional powder to a pre-alloyed MEA powder instead of doping the HEA with the element during alloying. This procedure enables a partial melting of the powder mixture at the desired brazing temperature and the formation of a HEA microstructure during isothermal solidification and homogenization phase during the brazing process.

Hence, this paper investigates whether the influence of additions of melting point depressing (MPD) elemental powder to the MEA brazing powder CoCrFeNi can lead to firm joints with a single-phase microstructure when brazing AISI304. The joints were brazed with varying parameters and the joint microstructure as well as the microhardness of the resulting braze metal were analyzed in order investigate the influence of the brazing parameters on the phase formation.

2 Materials

The MEA powder, consisting of equimolar proportions of Co, Cr, Fe, and Ni, was used as the base brazing alloy. The MPD was selected based on several criteria, including melting temperature, wetting behavior, and corrosion resistance. Furthermore, thermodynamic simulations were performed using Thermo-Calc prior to the brazing experiments to assess the suitability of the selected MPD by evaluating phase formation and the thermodynamic stability of the resulting alloy systems.

The MEA CoCrFeNi was produced via powder atomization and supplied by Chemnitz University of Technology. To investigate the influence of alloy composition on the properties of the resulting HEAs, the MPD was added to the MEA in different proportions. To ensure a homogeneous distribution of the constituent powders, the powder mixtures were blended in a tumbler mixer for 1 h. The compositions investigated in this study are summarized in Table 1.

Table 1
Composition of the HEA CoCrFeNi-MPD_x powder mixture

$CoCrFeNi\text{-}MPD_{20}$	**Co [at.-%]**	**Cr [at.-%]**	**Fe [at.-%]**	**Ni [at.-%]**	**MPD [at.-%]**
	20	**20**	**20**	**20**	**20**
$CoCrFeNi\text{-}MPD_{40}$	15	15	15	15	40
$CoCrFeNi\text{-}MPD_{80}$	5	5	5	5	80

A suitable MPD is tin as its melting temperature amounts only 231.9°C. In order to obtain a brazing paste, the B2 binder supplied by Innobraze GmbH was added to the powder mixture at a concentration of 40 wt.%. AISI 304 austenitic stainless steel (EN 1.4301, X5CrNi18-10) was selected as the base material for the brazing experiments due to its widespread industrial application and good corrosion resistance. The steel specimens had dimensions of 25 mm × 25 mm × 3 mm. Prior to brazing, the specimen surfaces were mechanically prepared by grinding with 600-grit SiC abrasive paper to remove surface oxides and ensure reproducible wetting conditions.

3 Experimental procedures

3.1 Brazing conditions

The brazing paste was applied to the steel plates by screen printing using a stencil with a thickness of 0.1 mm, resulting in a nominal brazing gap of 100 µm. Subsequently, a second steel plate was carefully positioned on top of the brazing paste layer to form the brazing assembly. During brazing, the assemblies were loaded with weights to ensure consistent contact between the joining partners and to maintain the predefined brazing gap. The geometry of the brazing assembly is illustrated in Fig. 1.

Brazing was carried out in a high-temperature vacuum furnace manufactured by Schmetz (model EU 80/1H), capable of achieving a vacuum level of 5.3×10^{-4} mbar. The specimens were brazed at temperatures of 1000°C and 1100°C, respectively. To ensure controlled binder removal and homogeneous heating, the specimens were subjected to a multi-stage heating cycle rather than being heated directly to the brazing temperature.

Initially, the specimens were heated to 120°C at a heating rate of 15 K min^{-1} and held for 15 min to remove residual moisture from both the specimens and the binder. Subsequently, the temperature was increased to 450°C at a heating rate of 40 K min^{-1} and maintained for 15 min to facilitate the evaporation of the organic binder constituents. A final intermediate temperature plateau was introduced at 850°C and 950°C for the brazing temperatures of 1000°C and 1100°C, respectively. These temperatures were reached at a heating rate of 50 K min^{-1} and held for 15 min to ensure a homogeneous temperature distribution throughout the brazing assembly.

Afterwards, the specimens were heated to the respective brazing temperatures of 1000°C or 1100°C and held for 60 min. Following the brazing cycle, rapid cooling was performed with nitrogen with an excess pressure of 2 bar in order to suppress a mutual formation of undesired intermetallic phases. An example of the temperature profile employed for brazing at 1100°C is shown in Fig. 2.

3.2 Microstructural characterization

The joint microstructures were examined using scanning electron microscopy (SEM). For this purpose, the specimens were sectioned perpendicular to the faying surfaces to enable detailed examination of the joint cross-section. The cross-sectional samples were subsequently mounted in EpoxiCure 2 epoxy resin, followed by grinding and polishing to obtain a surface suitable for microscopic investigation.

Prior to SEM analysis, the specimens were coated with a thin gold layer by sputter deposition to prevent surface charging during imaging. The microstructural investigations were conducted using a JEOL JSM-7001F scanning electron microscope.

3.3 Hardness determination

Hardness is a decisive factor in brazing, particularly with regard to the load-bearing capacity, wear resistance, and service life of the joint. To determine these mechanical properties, the hardness of the brazed joint was measured. This was carried out using the Vickers hardness test method. A Streurs Duramin 4.0 indentation tester was used for this purpose. To determine the hardness, the values in the formed phases were averaged across 7 measurement points and evaluated at a test force of 0.0981 N (HV0.01).

4 Results and discussion

Prior to the experimental investigations, thermodynamic simulations were performed using Thermo-Calc in combination with the TCHEA5 database. Phase diagrams of the MEA–MPD systems were calculated as a function of the MPD concentration to assess phase stability and predict phase formation.

One of the investigated alloy systems was the CoCrFeNi–Sn HEA. The influence of both the Sn content and the brazing temperature on the microstructure and properties of the brazed joints was examined. To support the experimental investigations, thermodynamic simulations were performed using Thermo-Calc in combination with the TCHEA5 database. Based on these simulations, a phase diagram of the CoCrFeNi–Sn system was calculated as a function of the Sn molar fraction. The resulting phase diagram is presented in Fig. 3.

The calculated binary phase diagram for the CoCrFeNi–Sn system shows complete solubility of the alloy in the liquid state and partial solubility in the solid state. During isothermal solidification of a tin-rich melt, the first CoCrFeNi-rich solid-solution crystals precipitate at a tin content below 48 at.-% Sn. At a tin content of 15 at.-% Sn, complete solidification finally occurs as a CoCrFeNi-rich solid solution, without the formation of any additional phases. At a brazing temperature of 1000°C, a BCC phase initially

precipitates at a tin content of 74 at.-% Sn, which subsequently dissolves again. After further phase transformations, the alloy finally solidifies completely isothermally as a CoCrFeNi-rich solid solution once the tin content falls below 8 at.-% Sn.

4.1 Microstructural characterization of CoCrFeNi-Sn_x

The microstructure of the brazed joints was characterized by SEM. In addition to a visual assessment of the joint morphology, energy-dispersive X-ray spectroscopy (EDS) was employed to analyze the elemental distribution within the brazed region. Figure 4 presents cross-sectional SEM images of brazed joints produced from AISI 304 stainless steel (EN 1.4301) using CoCrFeNi–Sn□ brazing alloys with different compositions and brazing temperatures.

A comparison of the CoCrFeNi–Sn_{20}, CoCrFeNi–Sn_{40}, and CoCrFeNi–Sn_{80} systems brazed at 1000°C (Fig. 4a–c) reveals that complete filling of the brazing gap was achieved only at high Sn contents. In contrast, brazing at 1100°C resulted in complete gap filling and the formation of continuous metallurgical bonds for all investigated compositions.

For the joints produced with CoCrFeNi–Sn_{20} and CoCrFeNi–Sn_{40} at 1000°C, only partial wetting of the brazing gap was observed. Residual powder particles remained visible within the joint and were surrounded by a solidified liquid phase, indicating incomplete melting and limited diffusion during brazing. In comparison, the CoCrFeNi–Sn_{80} alloy exhibited complete wetting and filling of the brazing gap at 1000°C. A bright, continuous phase was observed in the center of the brazed joint, which was intersected by several vertical cracks.

The joints brazed at 1100°C exhibited improved wetting behavior and a more homogeneous interaction between the brazing alloy and the base material. Similar bright phases were observed in the center of the brazed joints; however, these phases also contained cracks, indicating their brittle nature. The fraction of the bright phase decreased with increasing Sn content in the alloy, suggesting enhanced diffusion and homogenization between the CoCrFeNi–Sn alloy and the base material at higher Sn concentrations. EDS analysis of the CoCrFeNi-Sn_{80} joint revealed that the bright phases were enriched in Sn and Ni and is shown in Fig. 5.

Evaluation of the EDS elemental maps show that the brazed joint consisted of Sn-rich phases forming a distinct band in the center of the brazing gap. This central region was surrounded by Sn-depleted phases extending toward the base material. In contrast, Cr, Fe, and Co were distributed relatively uniformly throughout both the brazed joint and the adjacent base material.

Further information on the local chemical composition was obtained from EDS point analyses (Fig. 5a). The measured compositions at the selected locations are summarized in Table 2.

Table 2
Chemical composition (at.-%) at the locations indicated in Fig. 5a for the AISI 304 stainless steel (EN 1.4301)/CoCrFeNi–Sn80 brazed joint.

No.	Co [at.-%]	Cr [at.-%]	Ni [at.-%]	Fe [at.-%]	Sn [at.-%]	Mn [at.-%]
1	0.40	19.99	7.1	71.26	0.15	1.2
2	0.60	18.34	6.24	70.83	2.53	0.82
3	0.80	7.2	21.03	31.69	36.91	2.30
4	1.10	20.44	4.47	69.66	3.35	0.92
5	0.80	19.11	6.68	70.41	1.94	0.97
6	0.50	20.05	7.68	70.52	0.00	1.24

Phase A, corresponding to measurement point 3, is located in the center of the brazed joint and contains approximately 36 at.-% Sn and 21 at.-% Ni, while exhibiting a lower Fe content of approximately 31 at.-% compared with the surrounding phases. This composition indicates the formation of Sn–Ni-rich intermetallic phases.

Based on the measured elemental composition and the Ni–Sn phase diagram, these phases are likely associated to the Ni_3Sn_4, Ni_3Sn_2, or Ni_3Sn phase fields. Owing to the presence of Fe in the investigated alloy system, the formation of (Ni,Fe)-containing intermetallic compounds cannot be excluded. Such phases are expected to form preferentially at the interface between the Sn-rich liquid phase and the Ni-containing MEA. Due to the low melting temperature of Sn (232°C), Sn represents the dominant liquid constituent during brazing. The strong chemical affinity between Ni and Sn, combined with their negative enthalpy of mixing, promotes the dissolution of Ni into the liquid Sn phase and the subsequent formation of Sn–Ni intermetallic compounds.

Furthermore, the variations in elemental composition observed among the individual measurement locations suggest a certain degree of Fe incorporation into the intermetallic phase. Such substitutional solubility is consistent with the multicomponent nature of CoCrFeNi-based alloy systems.

Phase B, represented by measurement points 1, 2, 4, and 5, is characterized by comparatively low Sn and Ni contents and significantly higher concentrations of Fe and Cr. This composition is indicative of an Fe–Cr-rich matrix phase and suggests the formation of a solid-solution region dominated by these elements. Furthermore, the elevated Fe and Cr contents indicate substantial diffusion of these elements from the base material into the brazing alloy during the joining process.

The Fe/Cr ratio of approximately 3.4 is consistent with that of the base material (point 6), further supporting the interpretation of extensive elemental interdiffusion. Additional evidence for diffusion from the base material is provided by the presence of Mn at points 1–5. Since Mn is present only as an

alloying element in the AISI 304 stainless steel and not in the brazing alloy, its detection within the brazed joint confirms diffusion from the base material into the reaction zone. The formation of Sn–Ni-rich intermetallic phases lead to a significant consumption of Sn within the brazed joint. As a result, the amount of free liquid Sn available for further diffusion is reduced, limiting the penetration depth of Sn into the diffusion zone and the adjacent base material. Subsequent rapid cooling preserved this microstructural state by suppressing further phase transformations and diffusional homogenization.

Phase C corresponds to the unaffected base material. No detectable Sn and only negligible amounts of Co were found in this region, both of which are characteristic constituents of the brazing alloy. In contrast, the Mn concentration was noticeably higher, consistent with the composition of the AISI 304 stainless steel. The corresponding measurement location is situated outside the diffusion zone.

Comparable microstructural characteristics were identified in the CoCrFeNi–Sn□ systems with lower Sn contents brazed at 1100°C and in the CoCrFeNi–Sn_{80} system brazed at 1000°C. Although the same general phase evolution and interdiffusion behavior were observed, the extent of the diffusion zones varied and was, in some cases, less pronounced Following the microstructural characterization, the mechanical properties of the brazed joints were assessed by means of hardness measurements.

4.2 Mechanical properties

The hardness of the brazed joints was determined using the Vickers hardness test method (HV0.01). Hardness measurements were performed only on specimens almost complete gap filling, namely the CoCrFeNi–Sn□ systems brazed at 1100°C and the CoCrFeNi–Sn80 system brazed at 1000°C. The measured hardness values are presented in Fig. 6.

The hardness was evaluated separately for the microstructural regions identified in Section 4.1, including the Sn-rich phase (Phase A), the Sn-depleted phase (Phase B), and the unaffected base material (Phase C). A clear dependence of hardness on the Sn content was observed. Increasing the Sn concentration in the brazing alloy resulted in a decrease in hardness. For the CoCrFeNi–Sn20 system, a hardness of 895 ± 21 HV was measured, whereas the hardness decreased to 748 ± 34 HV for the CoCrFeNi–Sn80 system.

The brazing temperature also influenced the hardness of the investigated phases. For the CoCrFeNi–Sn80 system, a lower hardness was measured after brazing at the higher process temperature. At 1000°C, the hardness of the Sn-rich phase was determined to be 809 ± 103 HV. In addition, crack formation around the indentations was observed during hardness testing, indicating the brittle nature of these phases. The occurrence of cracking also reduced the reliability of the measurements and contributed to the comparatively large standard deviations.

From a mechanical perspective, the presence of these hard and brittle phases is considered unfavorable, as they are predominantly located in the center of the brazed joint. This region is typically subjected to the highest shear stresses during service, making it a potential site for crack initiation and premature failure of the joint under mechanical loading.

The decrease in hardness with increasing Sn content may be attributed to changes in the composition and distribution of the Sn–Ni-rich phases formed within the brazed joint. At higher Sn concentrations, the formation of Sn-rich intermetallic phases, such as those associated with the Ni_3Sn_4 phase field, becomes thermodynamically more favorable due to the excess availability of Sn.

The influence of brazing temperature suggests that lower processing temperatures promote the retention of a larger fraction of the phases formed during solidification. This effect may be further enhanced by the rapid cooling applied after brazing, which can suppress diffusional homogenization and preserve metastable microstructural features.

For Phase B, corresponding to the Sn-depleted region within the brazed joint, hardness increased with increasing Sn content. In contrast to Phase A, no significant influence of brazing temperature on hardness was observed. Instead, the hardness of this phase appeared to depend primarily on the alloy composition.

A pronounced hardness discontinuity was observed between the hard Sn-rich phase and the adjacent softer regions of the brazed joint. No gradual hardness transition or continuous hardness gradient was detected across the joint. Such an abrupt change in mechanical properties may lead to localized stress concentrations and is therefore considered mechanically unfavorable.

The base material exhibited nearly constant hardness values for all investigated conditions, indicating that the brazing process had no significant effect on its mechanical properties.

5 Conclusion

Overall, the results demonstrate that sound brazed joints can be produced between AISI 304 stainless steel (EN 1.4301) and CoCrFeNi–Sn brazing alloys. The microstructure and resulting properties of the joints were found to depend strongly on both the Sn content and the brazing temperature. Increasing the Sn concentration and the brazing temperature promoted improved wetting and diffusion, resulting in a more homogeneous microstructure within the brazed joint.

Furthermore, distinct Sn-rich and Sn-depleted regions were observed within the brazed joints. EDS analyses revealed significant elemental partitioning between these regions and indicated the formation of Sn–Ni-rich intermetallic phases in the central part of the joint. The presence and distribution of these phases were found to have a pronounced influence on the hardness and overall microstructural characteristics of the brazed joints.

Hardness measurements were performed to evaluate the mechanical properties of the brazed joints. The results showed that the hardness of the phases formed within the brazed joint was influenced by the brazing temperature. In addition, pronounced hardness variations were observed across the joint, which can be attributed to the heterogeneous phase distribution. Such abrupt changes in hardness may lead to

localized stress concentrations and are therefore considered detrimental to the mechanical performance of the joint.

However, the extent to which the observed phase formation affects the strength and failure behavior of the brazed joints remains to be investigated. Furthermore, additional research is required to determine how the formation of these phases can be minimized and how a more homogeneous joint microstructure can be achieved.

Although further optimization of the alloy system and process parameters is necessary, the investigated HEA brazing alloys demonstrated the ability to produce sound metallurgical joints. In particular, high Sn contents combined with elevated brazing temperatures resulted in improved joint quality, highlighting the considerable potential of these alloys for high-temperature brazing applications.

Declarations

Funding

The results presented in the manuscript were obtained within the project IGF 01IF23537N/1 funded by DLR and BMWE.

Competing interests

The authors have no competing interests to declare that are relevant to the content of this article.

Data availability

The data that support the findings of this study are available from the corresponding author upon reasonable request.

Author contributions

Laura Bültena and Lukas Wojarski contributed to the study conception and design. Material preparation, experiments, data collection and analysis were performed by Merle Hansen. The first draft of the manuscript was written by Laura Bültena supervised by Lukas Wojarski, and all authors commented on previous versions of the manuscript. Additions were made by Lukas Wojarski. All authors read and approved the final manuscript. Lukas Wojarski as project leader is responsible for the scientific approach.

References

1. Schuler V, Twrdek J (2019) Praxiswissen Schweißtechnik: Werkstoffe, Prozesse, Fertigung, 6., vollständig überarbeitete Auflage. Springer Vieweg, Wiesbaden
2. Guzmán I, Garza A, García F et al (2009) Brazing Process to Repair Wide Gap Cracks of Inconel 738 Superalloy Components. Materials Research Society symposia proceedings. Materials Research Society 1242. https://doi.org/10.1557/PROC-1242-S4-57
3. Way M, Willingham J, Goodall R (2020) Brazing filler metals. Int Mater Rev 65:257–285. https://doi.org/10.1080/09506608.2019.1613311
4. Dewangan SK, Mangish A, Kumar S et al (2022) A review on High-Temperature Applicability: A milestone for high entropy alloys. Eng Sci Technol Int J 35:101211. https://doi.org/10.1016/j.jestch.2022.101211
5. Yeh J-W, Chen S-K, Lin S-J et al (2004) Nanostructured High-Entropy Alloys with Multiple Principal Elements: Novel Alloy Design Concepts and Outcomes. Adv Eng Mater 6:299–303. https://doi.org/10.1002/adem.200300567
6. Zhang Y, Zuo TT, Tang Z et al (2014) Microstructures and properties of high-entropy alloys. Prog Mater Sci 61:1–93. https://doi.org/10.1016/j.pmatsci.2013.10.001
7. Hardwick L, Rodgers P, Pickering E et al (2021) Development of a Novel Ni-Based Multi-principal Element Alloy Filler Metal, Using an Alternative Melting Point Depressant. Metall Mater Trans A 52:2534–2548. https://doi.org/10.1007/s11661-021-06246-0
8. Zhang S, Wang T, Zhang G et al (2025) Current status of research on the application of high-entropy alloys in the field of brazing. Weld World 69:1705–1720. https://doi.org/10.1007/s40194-025-01991-x
9. Liu H-C, Tsai C-W (2021) Effect of Ge addition on the microstructure, mechanical properties, and corrosion behavior of CoCrFeNi high-entropy alloys. Intermetallics 132:107167. https://doi.org/10.1016/j.intermet.2021.107167
10. Miracle DB, Senkov ON (2017) A critical review of high entropy alloys and related concepts. Acta Mater 122:448–511. https://doi.org/10.1016/j.actamat.2016.08.081
11. Bridges D, Zhang S, Lang S et al (2018) Laser brazing of a nickel-based superalloy using a Ni-Mn-Fe-Co-Cu high entropy alloy filler metal. Mater Lett 215:11–14. https://doi.org/10.1016/j.matlet.2017.12.003
12. Tillmann W, Wojarski L, Stangier D et al (2020) Application of the eutectic high entropy alloy Nb0.73CoCrFeNi2.1 for high temperature joints. Weld World 64:1597–1604. https://doi.org/10.1007/s40194-020-00944-w
13. Tillmann W, Ulitzka T, Wojarski L et al Brazing of high temperature materials using melting range optimized filler metals based on the high-entropy alloy CoCrCuFeNi
14. Tillmann W, Ulitzka T, Wojarski L et al (2020) Development of high entropy alloys for brazing applications. Weld World 64:201–208. https://doi.org/10.1007/s40194-019-00824-y

Figures

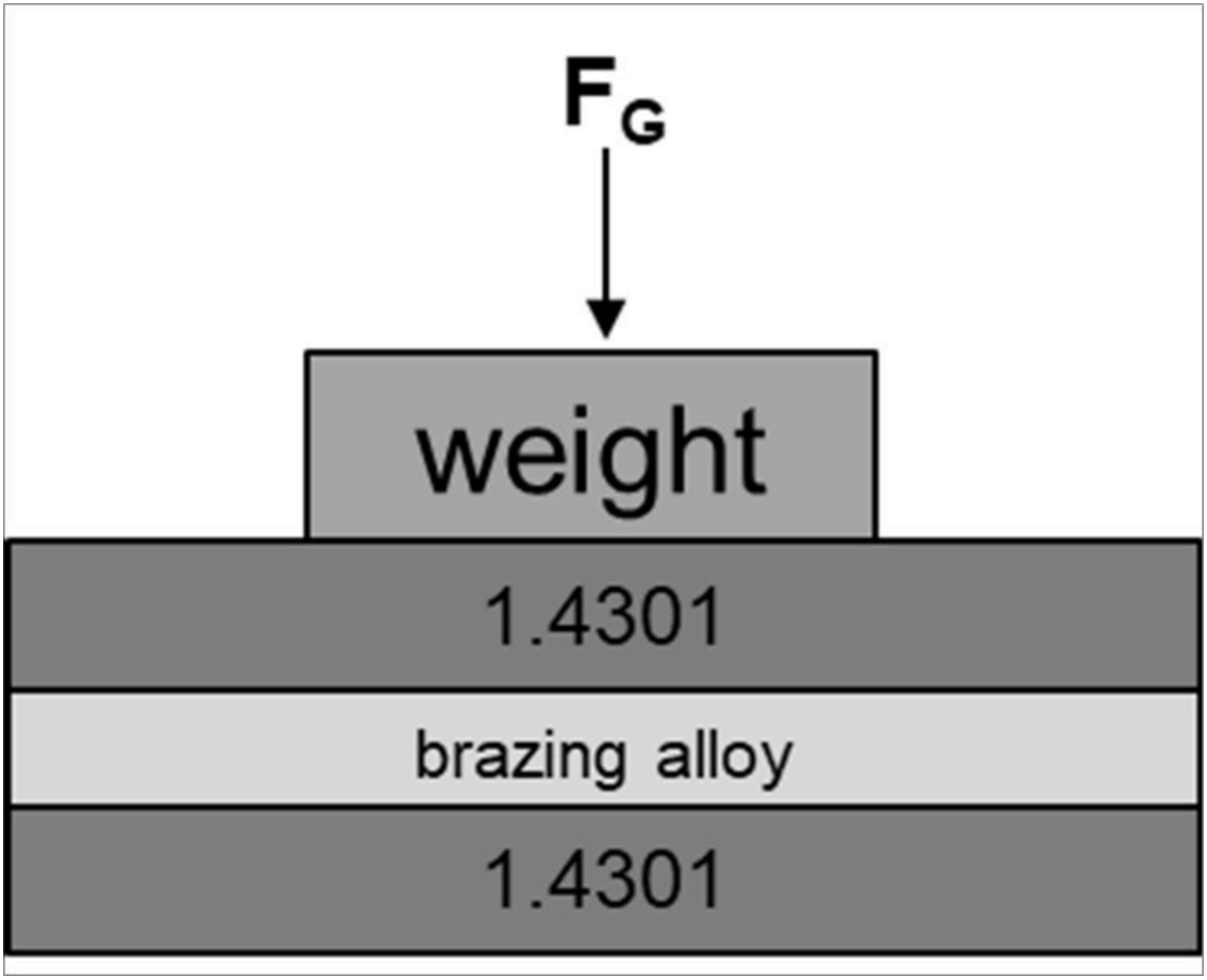


Figure 1

Sample geometry and application of brazing paste

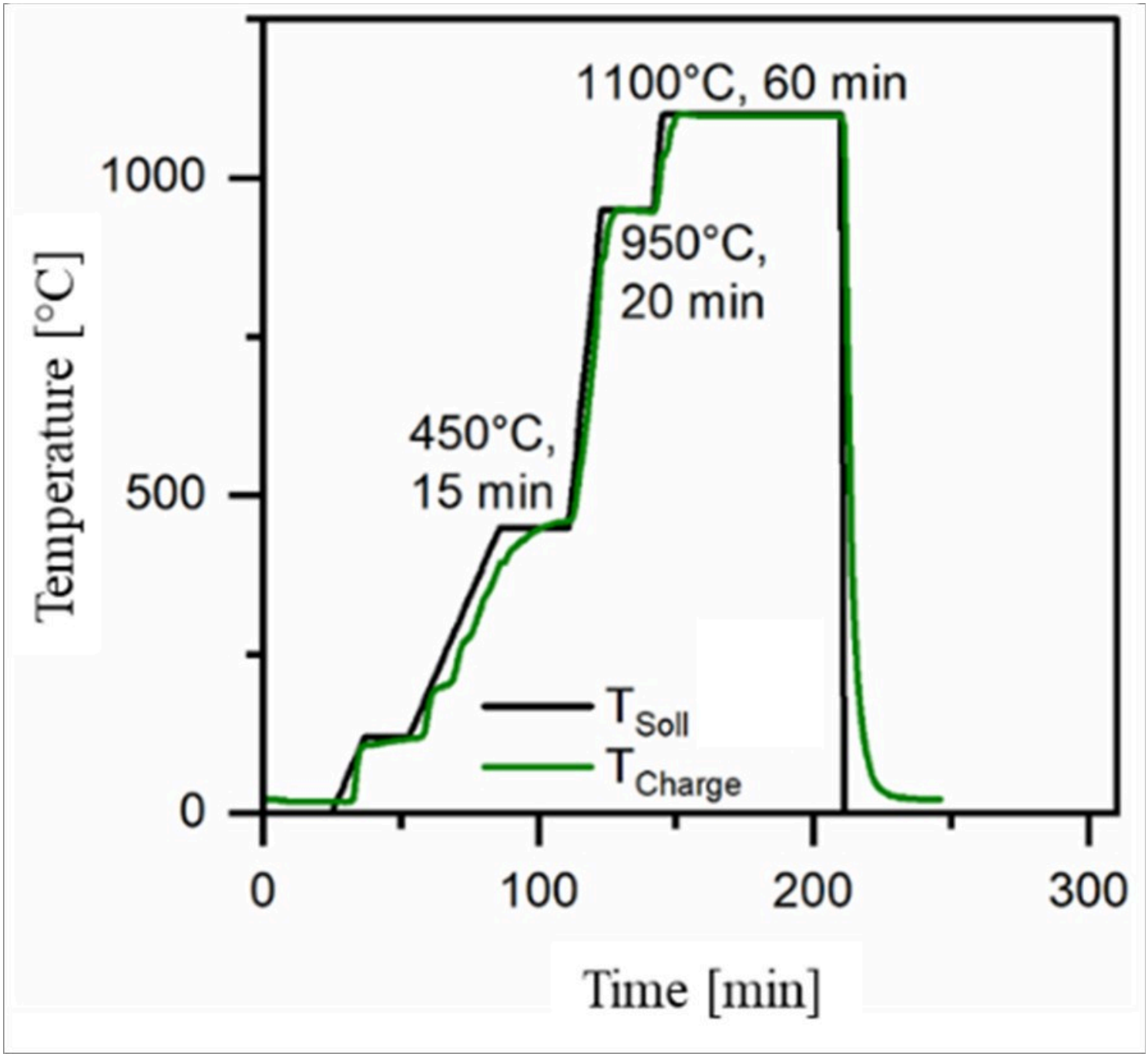


Figure 2

Temperature profile of the brazing process at 1100 °C

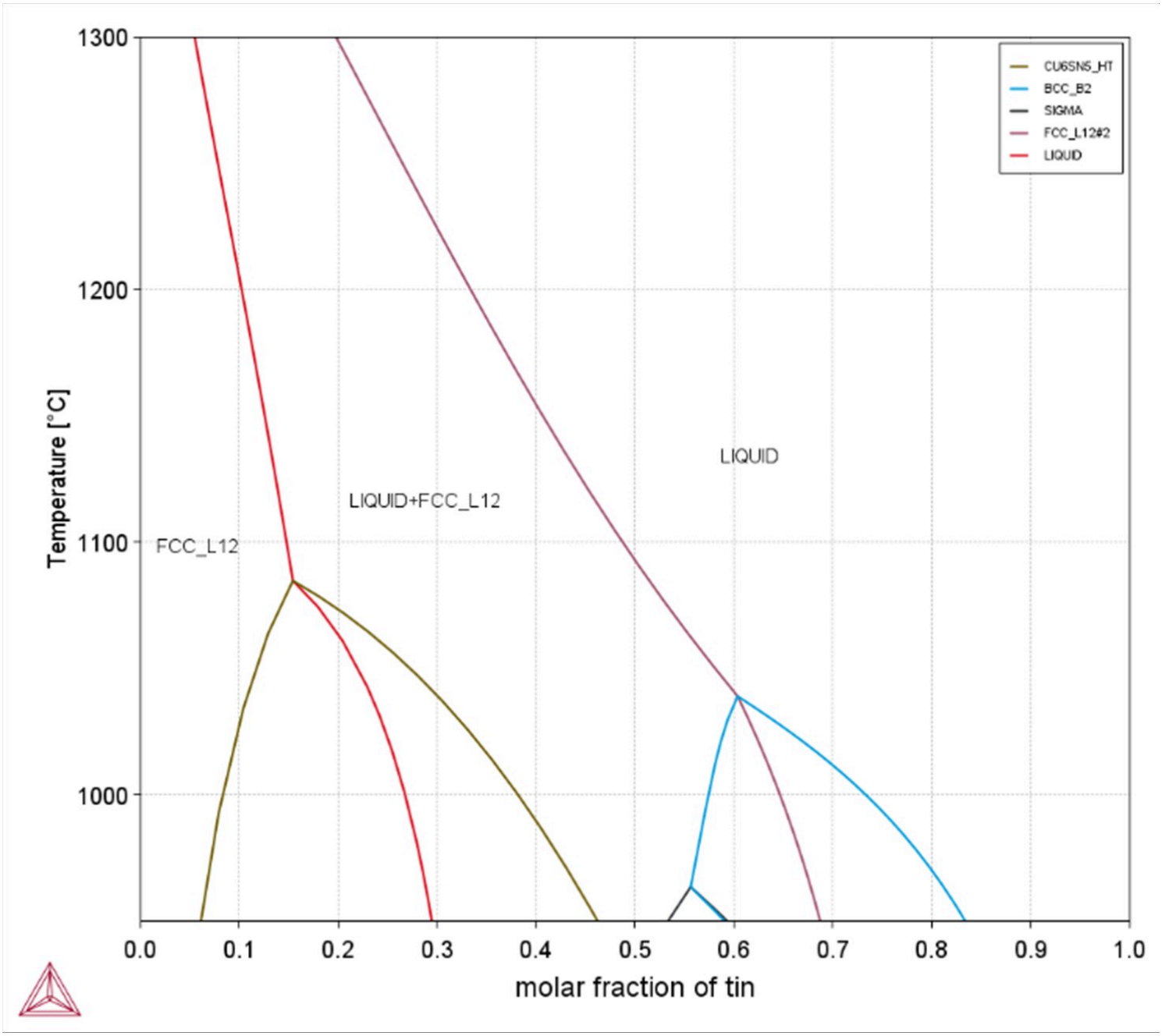


Figure 3

Phase diagram calculated using ThermoCalc

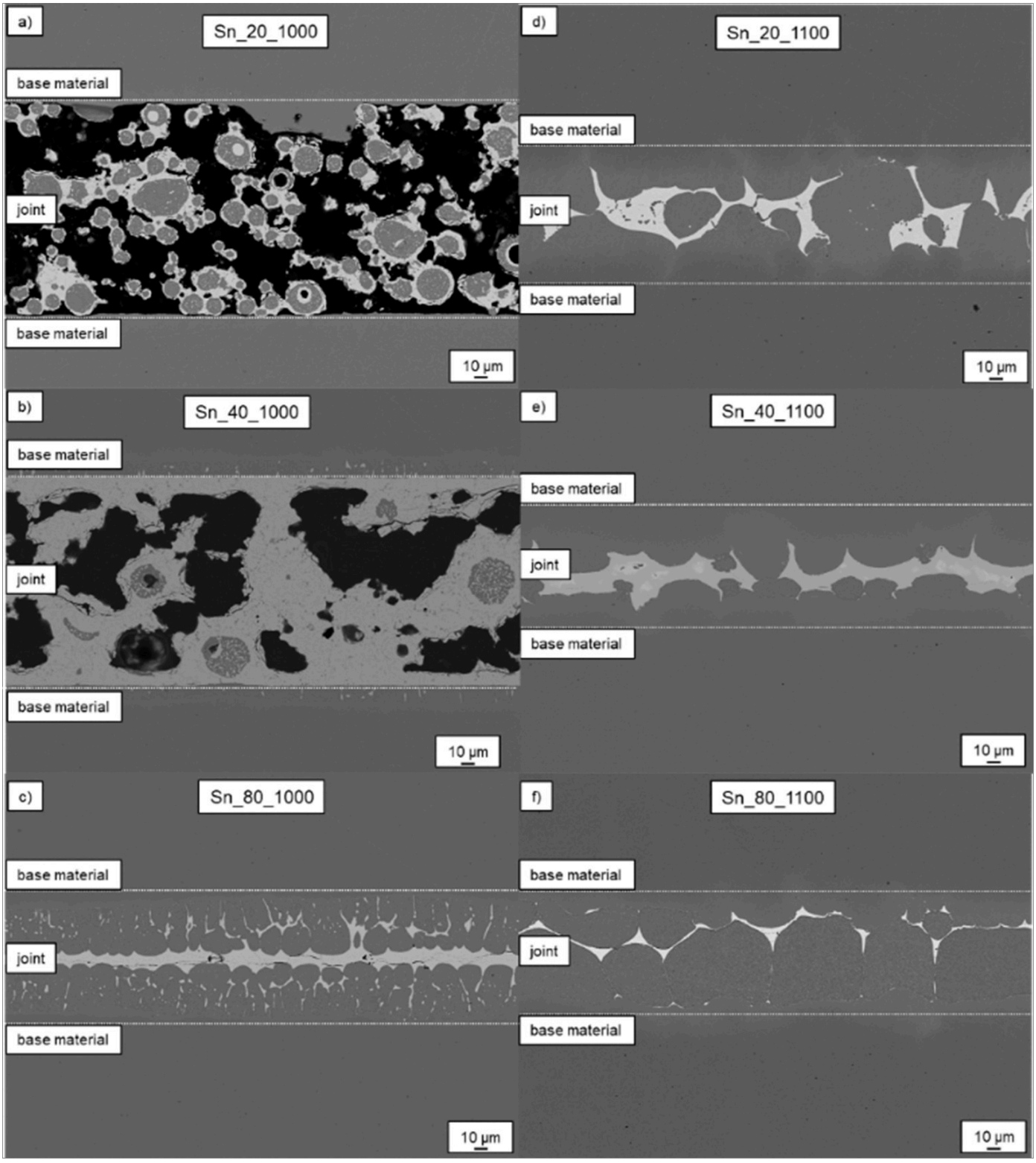


Figure 4

CoCrFeNi-Sn_x brazed joints at different temperatures and compositions. a) – c) CoCrFeNi-Sn_x brazed at 1000 °C; d) – f) CoCrFeNi-Sn_x brazed at 1100 °C

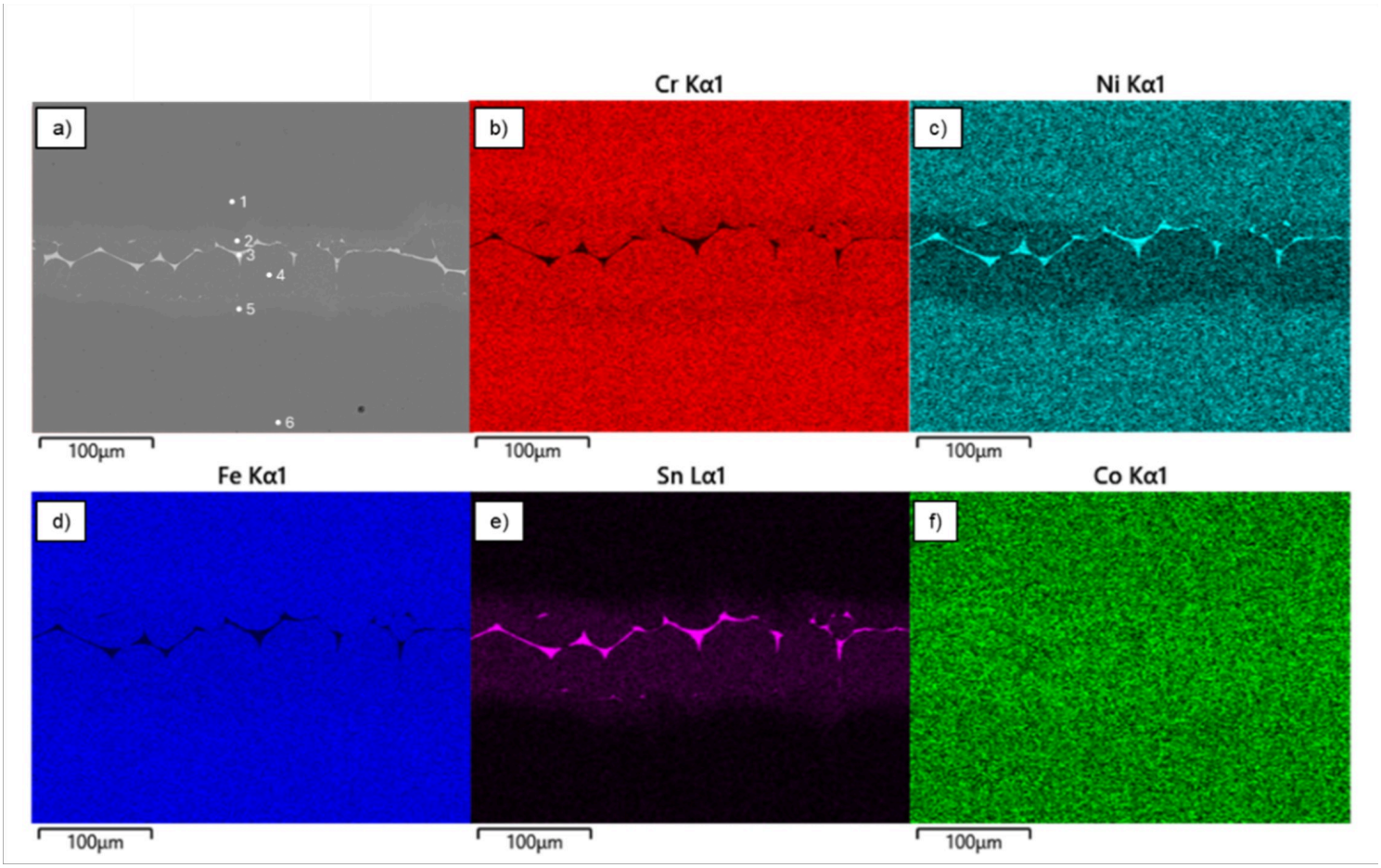


Figure 5

EDS elemental maps of the CoCrFeNi–Sn_{80} brazed joint: (a) SEM micrograph; (b) Cr distribution map; (c) Ni distribution map; (d) Fe distribution map; (e) Sn distribution map; and (f) Co distribution map

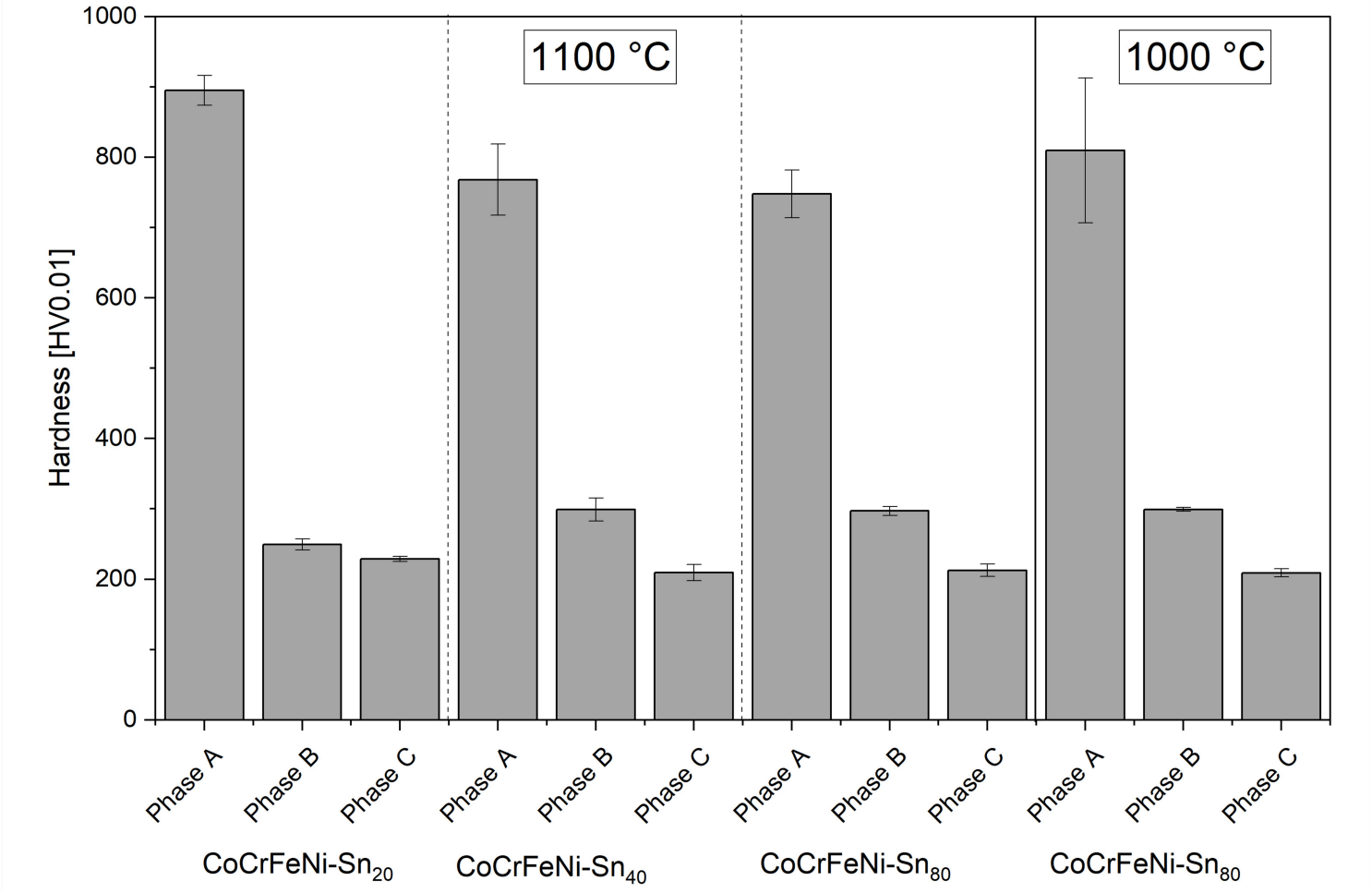


Figure 6

Vickers hardness (HV0.01) of CoCrFeNi–Sn brazing alloys at different brazing temperatures